Mineral. Deposita 31, 147–162 (1996)

MINERALIUM DEPOSITA

Sr, C and O isotope systematics in the Pucará Basin, central Peru

Comparison between Mississippi Valley-type deposits and barren areas

R. Moritz[1], L. Fontboté[1], J. Spangenberg[1], S. Rosas[2], Z. Sharp[3], D. Fontignie[1]

[1]Département de Minéralogie, Université de Genève, Rue des Maraîchers 13, CH-1211 Genève 4, Switzerland
[2]Arica 343, Lima 9, Chorrillos, Peru Escuela de Geologia, Universidad Nacional de Ingenieria, Lima, Peru
[3]Institut de Minéralogie, Université de Lausanne, CH-1015 Lausanne, Switzerland

Received: 26 April 1995/Accepted: 30 June 1995

Abstract. A combined Sr, O and C isotope study has been carried out in the Pucará basin, central Peru, to compare local isotopic trends of the San Vicente and Shalipayco Zn-Pb Mississippi Valley-type (MVT) deposits with regional geochemical patterns of the sedimentary host basin. Gypsum, limestone and regional replacement dolomite yield $^{87}Sr/^{86}Sr$ ratios that fall within or slightly below the published range of seawater $^{87}Sr/^{86}Sr$ values for the Lower Jurassic and the Upper Triassic. Our data indicate that the Sr isotopic composition of seawater between the Hettangian and the Toarcian may extend to lower $^{87}Sr/^{86}Sr$ ratios than previously published values. An ^{87}Sr-enrichment is noted in (1) carbonate rocks from the lowermost part of the Pucará basin, and (2) different carbonate generations at the MVT deposits. This indicates that host rocks at MVT deposits and in the lowermost part of the carbonate sequence interacted with ^{87}Sr-enriched fluids. The fluids acquired their radiogenic nature by interaction with lithologies underlying the carbonate rocks of the Pucará basin. The San Ramón granite, similar Permo-Triassic intrusions and their clastic derivatives in the Mitu Group are likely sources of radiogenic ^{87}Sr. The Brazilian shield and its erosion products are an additional potential source of radiogenic ^{87}Sr. Volcanic rocks of the Mitu Group are not a significant source for radiogenic ^{87}Sr; however, molasse-type sedimentary rocks and volcaniclastic rocks cannot be ruled out as a possible source of radiogenic ^{87}Sr. The marked enrichment in ^{87}Sr of carbonates toward the lower part of the Pucará Group is accompanied by only a slight decrease in $\delta^{18}O$ values and essentially no change in $\delta^{13}C$ values, whereas replacement dolomite and sparry carbonates at the MVT deposits display a coherent trend of progressive ^{87}Sr-enrichment, and ^{18}O- and ^{13}C-depletion. The depletion in ^{18}O in carbonates from the MVT deposits are likely related to a temperature increase, possibly coupled with a ^{18}O-enrichment of the ore-forming fluids. Progressively lower $\delta^{13}C$ values throughout the paragenetic sequence at the MVT deposits are interpreted as a gradually more important contribution from organically derived carbon. Quantitative calculations show that a single fluid-rock interaction model satisfactorily reproduces the marked ^{87}Sr-enrichment and the slight decrease in $\delta^{18}O$ values in carbonate rocks from the lower part of the Pucará Group. By contrast, the isotopic covariation trends of the MVT deposits are better reproduced by a model combining fluid mixing and fluid-rock interaction. The modelled ore-bearing fluids have a range of compositions between a hot, saline, radiogenic brine that had interacted with lithologies underlying the Pucará sequence and cooler, dilute brines possibly representing local fluids within the Pucará sequence. The composition of the local fluids varies according to the nature of the lithologies present in the neighborhood of the different MVT deposits. The proportion of the radiogenic fluid in the modelled fluid mixtures interacting with the carbonate host rocks at the MVT deposits decreases as one moves up in the stratigraphic sequence of the Pucará Group.

Carbonate-hosted Mississippi Valley-type (MVT) lead-zinc deposits are generally viewed as being an integral part of the evolution of a sedimentary basin. It is commonly accepted that these deposits are formed by brines, produced during burial of basinal sediments, that migrate along permeable aquifers and deposit metals in platform carbonate host rocks (e.g., Sverjensky 1984, 1986; Leach and Rowan 1986: Anderson and Macqueen 1988; Sangster 1990). Migration of these brines may also cause dolomitization, which is a conspicuous wallrock alteration feature in many MVT deposits (e.g., Beales and Hardy 1980). However, dolomitization is generally not restricted to only mineralized areas, as dolomite can appear at various stages during the development of a sedimentary basin, and can be precipitated from different types of fluids (e.g., Machel and Mountjoy 1986; Banner et al. 1988; Ghazban et al. 1992).

Sr isotope geochemistry is a powerful tool for characterizing the nature and the source of fluids from which carbonates were deposited in diverse geologic environments, as well as to pinpoint the relative timing of diagenetic events in sedimentary basins, including ore-formation (e.g., Kessen et al. 1981; Machel 1987; Gorzawski et al. 1989; Kaufman et al. 1990, 1991; Mountjoy et al.

1992). Thus, Sr isotope systematics, along with O and C isotopes, are particularly useful in constraining the relationship between the fluids precipitating carbonates at various stages in the lifetime of a sedimentary basin, and in understanding the evolution of these fluids during diagenesis.

This study was undertaken in the southern part of the Pucará basin, central Peru, an extensive carbonate platform hosting MVT deposits and occurrences (Fig. 1). It is a regional-scale follow-up of a local investigation of the San Vicente Zn-Pb MVT deposit carried out by Fontboté and Gorzwaski (1990). Five different profiles from the southern Pucará basin have been investigated in this study. From southwest to northeast, these profiles are located at Tingocancha, Malpaso, Tarma, Shalipayco and San Vicente (Figs. 1 and 2). Carbonates and sulfates from ore-bearing and barren areas, and from different positions in the stratigraphic column have been analyzed for their Sr, C and O isotope composition. The studied samples represent different subsequent evolution stages of the basin. Samples from barren areas include: (1) gypsum from marine evaporite lenses, (2) limestone and regional replacement dolomite proximal and distal to the contact with underlying detrital rock units, and (3) late-stage coarse crystalline calcite in cross-cutting veinlets near the contact with the underlying detrital rock units. Samples from ore-bearing areas are: (1) ore-stage, replacement dolomite, (2) white sparry dolomite, and (3) late-stage, void-filling, sparry calcite. For the sake of simplicity, ore-stage sparry dolomite and sparry calcite are grouped under the term sparry carbonates. The main features of the samples of this study are summarized in Table 1.

The present study focuses on the relationship between the fluids that formed MVT deposits in the Pucará basin, and fluids involved in late diagenetic processes in unmineralized parts of the basin. The purpose of this investigation is to determine how the local Sr, O and C isotopic trends of MVT deposits are related to regional geochemical patterns of the host sedimentary basin. We applied quantitative modelling of the isotopic trends in order to constrain the nature of the fluids and possible mixing processes in both barren areas and MVT deposits. The present regional investigation is complemented by a detailed local geochemical research devoted to the San Vicente District (Spangenberg, 1995).

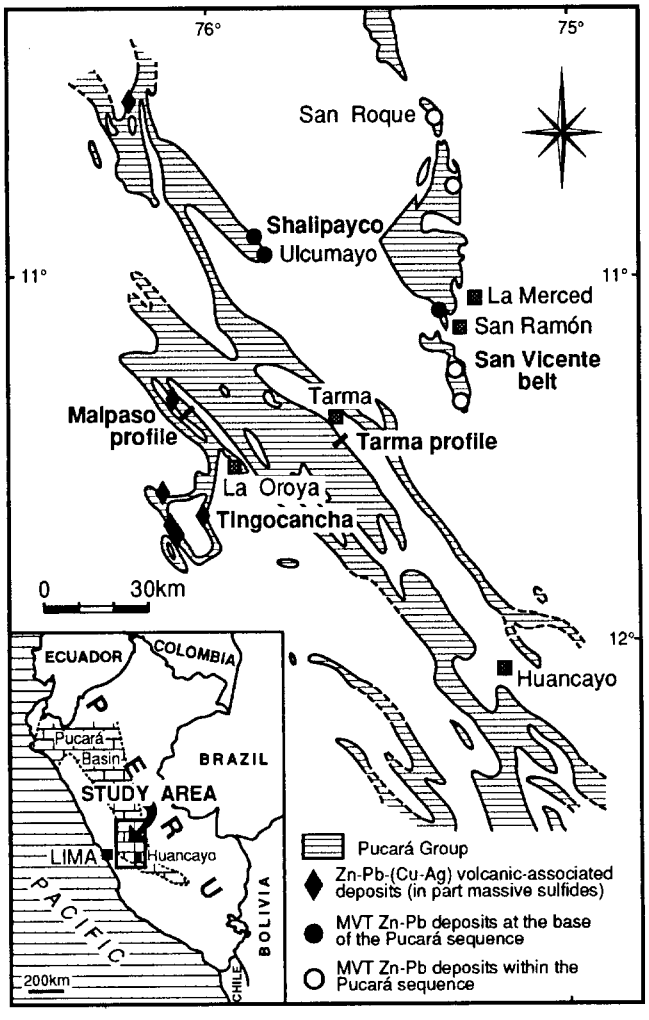

Fig. 1. Outcrop map of the Pucará Group (modified after Fontboté and Gorzawski 1990) with location of major ore deposits, and investigated profiles in this study (*bold*). The *inset* shows the total extension of the Pucará Basin and the location of the study area

Geological setting

The NNW-SSE trending Pucará basin is located on the western margin of the Brazilian Shield in northern and central Peru (Fig. 1). Regional aspects of the Pucará Group are described in Mégard (1978, 1987), Szekely and Grose (1972), Loughman and Hallam (1982), Prinz (1985a,b), Fontboté (1990), and Rosas (1994). A schematic profile of the southern part of this basin is shown in Fig. 2. The Pucará Group is subdivided from base to top into three formations (Figs. 2 and 3): (1) the Norian to Rhaethian Chambará Formation, consisting of up to 1200 m of thick dolomite and cherty limestone, (2) the about 100 m thick Hettangian to Sinemurian Aramachay Formation, composed of bituminous shale and sandstone, chert and phosphatic rocks, and (3) the Pliensbachian to Toarcian Condorsinga Formation consisting mainly of about 350 m thick limestone. Shallow water deposits, including peritidal facies with evaporite development and abundant oolithic barriers, predominate across the entire basin, except in the Aramachay Formation, which is characterized mainly by deeper anoxic facies.

The Upper Triassic-Lower Jurassic Pucará Group was deposited at the beginning of the Andean cycle. It mainly overlies magmatic and continental clastic sedimentary rocks of the Late Permian to Early Triassic Mitu Group (Mégard 1978, 1987; Carlier et al. 1982). The Mitu Group was likely deposited in an ensialic rift basin as indicated by the alkaline to sub-alkaline magmatic rocks underlying the central and western part of the Pucará basin (Kontak et al. 1985; Mégard 1987). During Late Permian-Triassic time, various igneous bodies of monzodioritic, granodioritic to granitic composition were emplaced in the Mitu Group basins and their margins (Capdevila et al. 1977; Carlier et al. 1982; Kontak et al. 1985). In the southwestern part (Fig. 2), the Pucará Group directly overlies weakly metamorphosed phyllites and quartzitic beds of the Lower to Middle Paleozoic Excelsior Group (Mégard 1978; Kobe 1990).

In the San Vicente area, in the northeastern part of the area under study (Fig. 2), the oldest rocks are mica schists and gneisses of probable Precambrian age (Mégard 1987). They are overlain by Paleozoic units comprised of metaclastic and carbonate rocks. The Upper Permian to Lower Triassic Mitu Group consists of continental conglomerates and sandstones, but without the volcanic rocks present in the western part of the basin (Mégard 1978; Fontboté and Gorzawski 1990). A Red Sandstone unit consisting of clastic rocks, probably derived from the emergent Brazilian shield, was deposited above the Mitu Group. This unit contains abundant gypsum

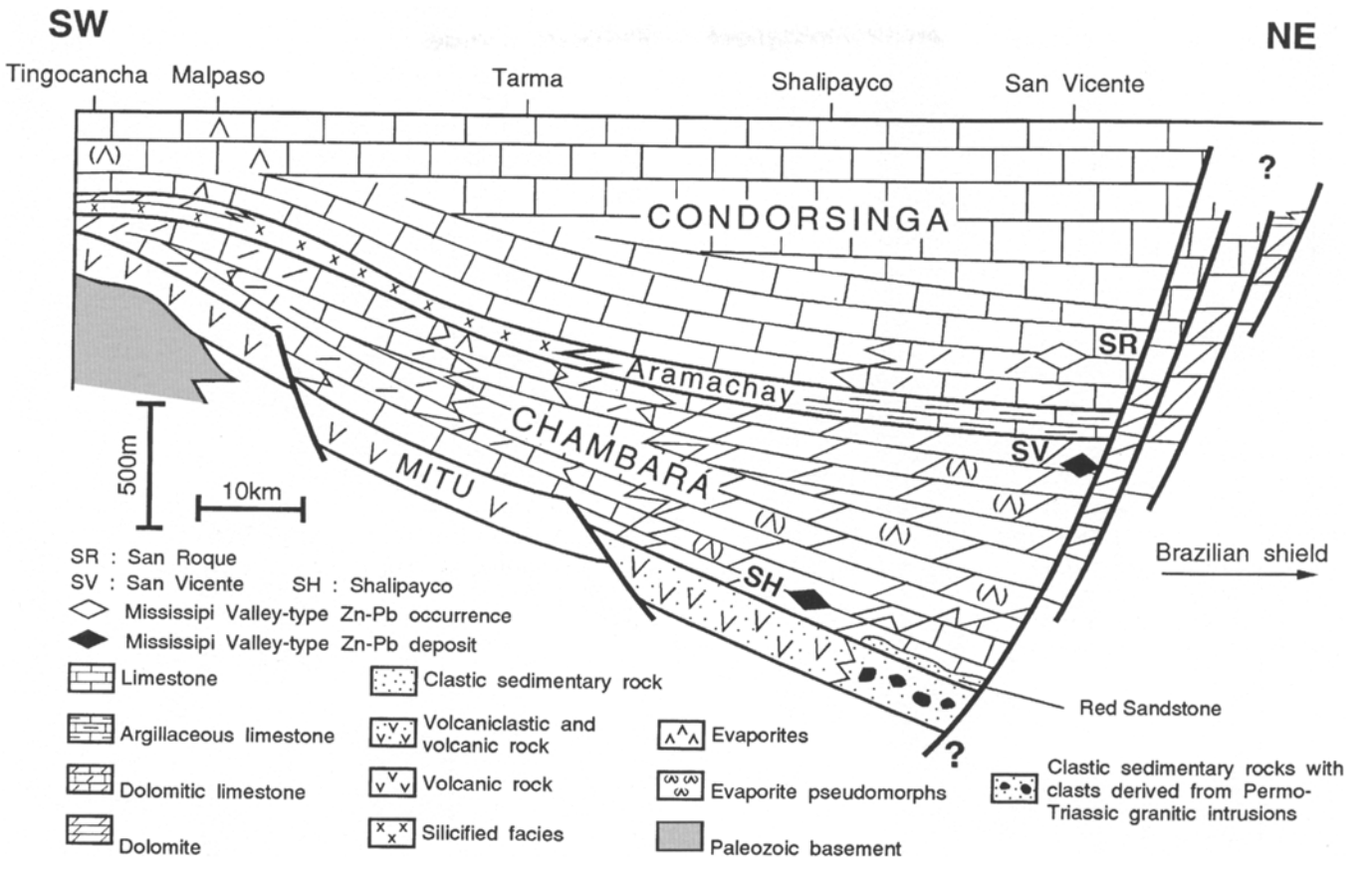

Fig. 2. Synthetic cross section of the southern Pucará basin (from Rosas 1994) with the location of the investigated profiles in this study (Tingocancha, Malpaso, Tarma, Shalipayco and San Vicente)

intercalations and is interdigitated with the carbonate rocks of the Chambará Formation. It is considered as part of the Pucará Group by Fontboté and Gorzawski (1990) and may represent an equivalent of the "Lower Sarayaquillo Formation" as defined by Mégard (1978).

The Pucará basin, as a large shallow-water carbonate platform, occupies a unique position among Andean basins. In its eastern part, it hosts the sole economic Andean Zn-Pb MVT deposits (Fig. 1). The Zn-Pb Shalipayco deposit is located at the base of and within the carbonate sequence (Fig. 3D), and was mined in the 1970s. It has an accumulated production and proven reserves of about 200 000 metric tons of ore, and grades of 8% Zn and 2% Pb, as well as 3 oz Ag per ton in the ore concentrate. The dominant ore minerals are sphalerite and galena with traces of pyrite and marcasite. The stratiform Zn-Pb orebodies at Shalipayco are in dolomitic rocks deposited in peritidal environments, with the lowest orebody occurring within a few meters above the contact with volcaniclastic rocks of the Mitu Group. Algal mats and evaporite pseudomorphs occur in mantos about 200 m above the Mitu-Pucará contact. Comparable ore showings run for about 20 km southward to the Ulcumayo mine (Fig. 1).

The MVT deposit at San Vicente is one of the largest Zn producers of Peru with an accumulated production of about 14 million metric tons of ore, reserves exceeding 4 million metric tons of ore, and Zn and Pb grades of 11% and 0.8%, respectively, with no Ag. The dominant ore minerals are sphalerite and galena with traces of pyrite and marcasite. Geologic and genetic aspects of this deposit are discussed in Fontboté and Gorzawski (1990). The San Vicente mine and smaller Zn-Pb-(F-Ba) occurrences form a 200 km long, north–south trending belt in the eastern Pucará basin, and are hosted mainly by the Chambará Formation. The main ore horizons are dolomitized oolithic grainstones of the barrier facies, and adjacent dolomitized tidal flat and lagoonal facies with cryptalgal laminations and evaporite molds. A large part of the ore displays a characteristic rhythmic banding between sulfide minerals and different generations of dolomite.

The age of the MVT deposits is not known precisely. At San Vicente, the MVT deposit is clearly cut by the major Andean thrust phases which started at about 20 Ma (Mégard 1987). Current models for the genesis of MVT deposits suggest a genetic link between foldbelt tectonism and the migration of the ore-bearing brines in sedimentary basins (e.g., Leach and Rowan 1986; Kesler 1994). Assuming a similar relationship between Andean tectonics and ore-bearing brine migration in the Pucará basin, the age of the MVT deposits could correspond to the first important uplift movements in the western Cordillera at about 100 Ma, but more probably to the first important orogenic movements affecting the high plateaus corresponding to the Incaic Phase at about 40 Ma (see Mégard 1987).

Analytical procedures

Samples of carbonates were obtained by drilling roughly polished hand specimens. About 200 mg of powdered material were extracted for each sample. Sr was extracted from carbonate samples of about 50 to 100 mg of the powdered material by leaching in cold 1 N HCl for 15 minutes with stirring. A ^{84}Sr spike was added to the acid prior to leaching for isotope dilution analysis. Gypsum samples were leached overnight in 2.5 N HCl at 80 °C. The dry residue of both carbonates and gypsum was dissolved in 2.5 N HCl, centrifuged and

Table 1. Summarized sample description

Rock type	Field and petrographic description	Lithological unit	Location and sample number
Evaporite	Massive sedimentary, mostly laminated gypsum Evaporite lenses intercalated with carbonate rocks deposited in shallow subtidal environments	Base of Pucarà Group Condorsinga	San Vicente: FSV-473 Tingocancha: SAC-3 and CUT-1; Malpaso: PAC-1, MAL-3 and FPE-77
Limestone	Slightly recrystallized and/or dolomitized	Lower Chambará	Tingocancha: PB-1; Malpaso: MAL-14; Tarma: PC-2 and PC-4; Shalipayco: FSH-27
	Diagenetic alteration absent to moderate	Upper Chambará	Tingocancha: PB-105; Malpaso: PA-145 and PA-157; Shalipayco: FSH-76, FSHJ-54 and FSHJ-73
	Bituminous silty limestone	Aramachay	Shalipayco: FSHJ-49
Regional replacement dolomite	Fine-grained, dark gray rock showing relict primary depositional features in places Restricted to particular facies: · Pack-grainstone	Chambará Aramachay	Malpaso: PA-16, PA-38 and PA-86; Shalipayco: FSH-64 and FSHJ-68 Tingocancha: PB-46
	· Mudstone	Chambará	Malpaso: PA-11, PA-12, PA-13 and PA-77; Tarma: FPE-78-3
	· Stromatolite	Chambará	Malpaso: PA-83
Ore-stage replacement dolomite	Fine-, medium- and coarse-crystalline dark gray color dolomite	Chambará	Shalipayco: FSH-13, FSH-19, FSH-71 and FSH-72; San Vicente: see Dolomite generation I in Fontboté and Gorzawski (1990)
Sparry dolomite	Late dolomitization: coarse to very coarse subhedral crystals of gray to white color dolomite. Occurs as mm- to cm-sized spots in, or as bands rhythmically interlayed with the earlier dark ore-bearing replacement dolomite	Chambará	Shalipayco: FSH-19; San Vicente: see Dolomite generation II in Fontboté and Gorzawski (1990)
Coarse-crystalline calcite	Coarse- to very coarse-crystalline xenomorphic fillings of calcite in pores and veinlets crosscutting replacement dolomite.	Chambará	Tingocancha: PB-1; Malpaso: PA-12 and PA-13
	Late state coarse-crystalline calcite in ore-bearing samples	Chambará	Shalipayco: FSH-19 and FSH-72 (evaporite pseudomorphs) San Vicente: FSV-052 (from Fontboté and Gorzawski 1990)

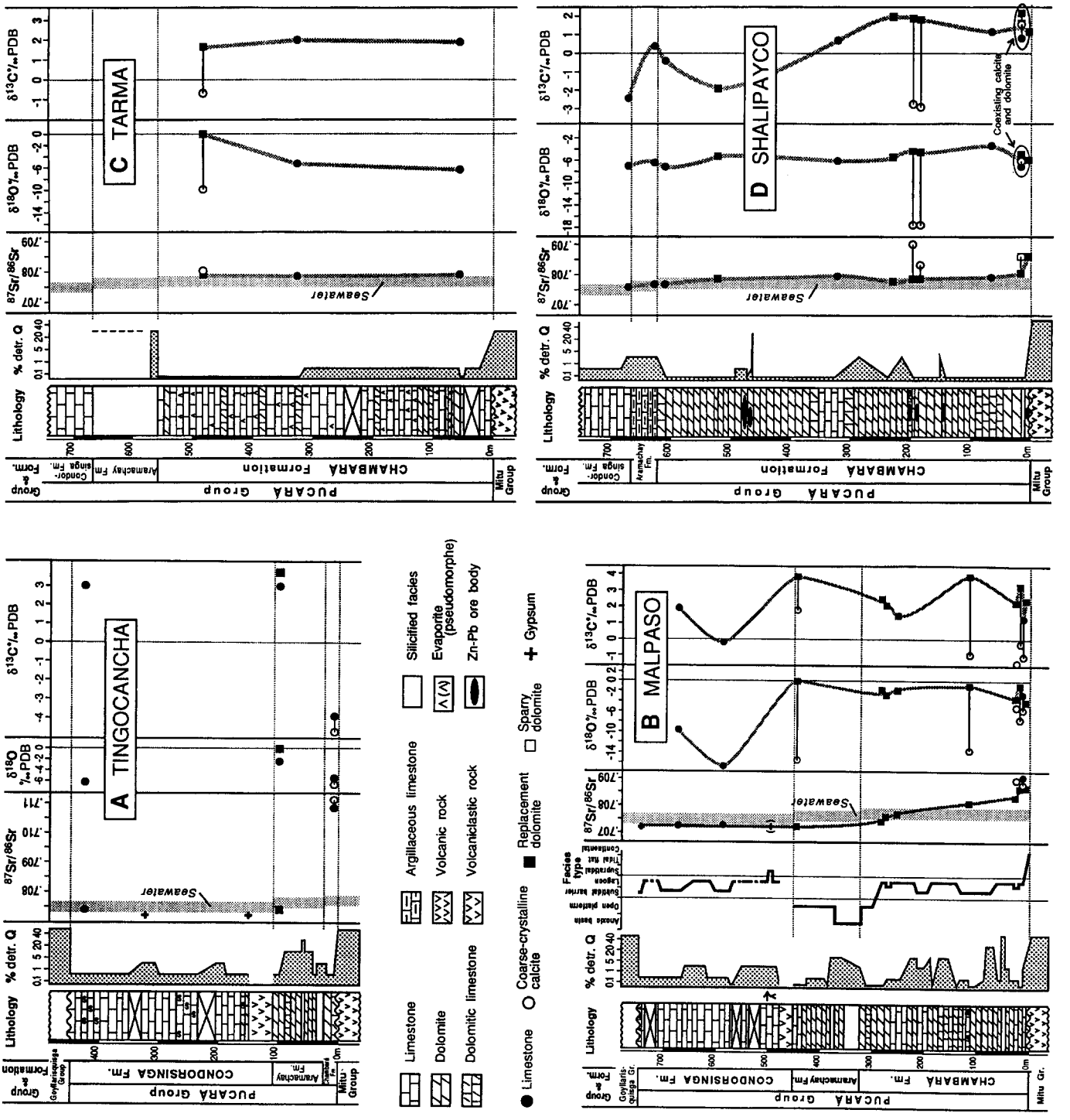

Fig. 3A–D. Profiles of the Pucará basin with Sr, O and C isotopic trends at **A** Tingocancha, **B** Tarma, **C** Malpaso and **D** Shalipayco

Sr was separated in HCl cation exchange columns. The samples were loaded on a double Re filament. Sr isotopic compositions were measured on a 7 collector Finnigan MAT 262 thermal ionization mass spectrometer at the University of Geneva. Analyses were performed by isotopic dilution and the $^{87}Sr/^{86}Sr$ ratios were calculated by the double spike method of Russel (1977). In-run errors are below 0.00003 2σ. Measured blanks for the procedure are negligible giving uncertainties significantly lower than in-run errors. The average value of the NBS 987 standard during the course of this study was 0.710242 ± 0.000005 1σ ($n = 83$).

C and O isotope analyses were performed following standard CO_2 extraction techniques of McCrea (1950). Approximately 15 mg of each sample were reacted with 100% H_3PO_4 at 25 °C for calcite and 50 °C for dolomite. The isotopic composition of carbonate samples with coexisting calcite and dolomite was determined following a selective extraction procedure modified after Al-Aasm et al. (1990). The cryogenically cleaned CO_2 gas was analyzed for C and O isotopic compositions on a Finnigan MAT 251 mass spectrometer at the University of Lausanne. Data were corrected for kinetic fractionation between H_3PO_4 and carbonates using fractionation

factors of 1.01025 for calcite (Friedman and O'Neil 1977) and 1.01177 for dolomite (Rosenbaum and Sheppard 1986). Data are reported as per mil (‰) deviations relative to the Pee Dee Belemnite (PDB) standard. Reproducibility was monitored through repeated analyses of laboratory standard samples, and is better than ± 0.05‰ and ± 0.1‰ for $\delta^{13}C$ and $\delta^{18}O$ values, respectively.

Strontium isotope data

Results

The isotope data are summarized in Table 2 and presented in Figs. 3, 4 and 5. Most of the gypsum, limestone and

Table 2. Sr, C and O isotopic data, Sr concentrations, % dolomite and location of the sedimentary rock samples from the Pucará basin

Sample	Rock type and Carbonate generation	Lithological unit (formation)	Height (m)	Calcite $\delta^{13}C$ (‰, PDB)	Calcite $\delta^{18}O$ (‰, PDB)	Dolomite $\delta^{13}C$ (‰, PDB)	Dolomite $\delta^{18}O$ (‰, PDB)	$^{87}Sr/^{86}Sr$	2σ	Sr (ppm)	% dolomite
Tingocancha											
PB-1	Limestone (I)	Chambará	0.2	− 3.9	− 5.7			0.71083	1	114	30
	Coarse calcite (II)	Chambará	0.2	− 4.8	− 6.9			0.71117	2	157	30
PB-46	Limestone-Repl. Dol (I)	Aramachay	98.1	3.0	− 2.4	3.7	− 0.2	0.70734	4	79	94
Sac-3	Gypsum	Condorsinga	150					0.70718	2		
Cut-1	Gypsum	Condorsinga	325					0.70720	3		
PB-105	Limestone (I)	Condorsinga	423.7	2.9	− 6.4			0.70741	2	177	2.6
Malpaso											
PA-11	Repl. Dol (I)	Chambará	9.4			2.3	− 4.3	0.70866	2	103	89
PA-12	Limestone (I)	Chambará	12.4	1.1	− 2.8			0.70907	3	155	38
	Coarse calcite (II)	Chambará	12.4	− 1.1	− 5.9			0.70878	4	137	0
PA-13	Repl. Dol (I)	Chambará	17.1			3.1	− 1.1	0.70866	2	134	61
	Coarse calcite (II)	Chambará	17.1	− 0.3	− 7.5						0
MAL-14	Limestone (I)	Chambará	24	− 1.7	− 5.1			0.70893	1		< 10
PA-16	Repl. Dol (I)	Chambará	25			2.2	− 3.4	0.70831	3	125	74
PA-38	Repl. Dol (I)	Chambará	112.2			3.7	− 0.9	0.70813	2	93	65
	Coarse calcite (II)	Chambará	112.2	− 1.0	− 13.7						0
PA-77	Repl. Dol (I)	Chambará	253.3			1.4	− 1.7	0.70768	2	68	88
PA-83	Repl. Dol (I)	Chambará	278			2.0	− 2.8	0.70760	1	72	93
PA-86	Repl. Dol (I)	Chambará	280.9			2.3	− 2.2	0.70746	3	80	94
Pac-1	Gypsum	Condorsinga	490					0.70725	7		
PA-145	Limestone (I)	Condorsinga	584.8	− 0.2	− 16.6			0.70729	2	120	4
PA-157	Limestone (I)	Condorsinga	666.2	1.9	− 9.8			0.70726	3	160	3
MAL-3	Gypsum	Condorsinga	745					0.70723	2		
FPE-77	Gypsum	Condorsinga	745					0.70720	6		
Tarma											
PC-2	Limestone (I)	Chambará	55.3	1.9	− 6.6			0.70787	2	322	8
PC-4	Limestone (I)	Chambará	328.5	2.0	− 5.3			0.70784	2	266	4
FPE-78-3	Repl. Dol (I)	Chambará	485			1.6	0.1	0.70788	2	115	89
	Coarse calcite (II)	Chambará	485	− 0.7	− 10.1			0.70800	2	151	0
Shalipayco											
FSH-13	Repl. Dol (I)	Chambará	1.5			1.1	− 6.3	0.70857	2	86	89
FSH-19	Limestone-Repl. Dol (I)	Chambará	1.5	0.8	− 7.1	2.1	− 5.2	0.70799	3	79	
	Coarse calcite-Sparry Dol (II)	Chambará	1.5	1.5	− 5.2	1.6	− 6.2	0.70853	5	67	
FSH-27	Limestone (I)	Chambará	62	1.1	− 3.7			0.70788	4	1576	16
FSH-71	Repl. Dol (I)	Chambará	192			1.9	− 4.6	0.70789	4	107	83
	Coarse calcite (II)	Chambará	192	− 2.8	− 18.0			0.70898	5	66	
FSH-72	Repl. Dol (I)	Chambará	192			1.8	− 4.8	0.70786	1	119	83
	Coarse calcite (II)	Chambará	192	− 2.9	− 17.9			0.70830	2	165	
FSH-64	Repl. Dol (I)	Chambará	230			2.0	− 5.6	0.70780	6	50	94
FSH-76	Limestone (I)	Chambará	318	0.7	− 6.2			0.70790	1	221	5
FSH-68	Repl. Dol (I)	Chambará	519			1.9	− 5.3	0.70773	2		> 90
FSHJ-73	Limestone (I)	Chambará	607	0.3	− 7.1			0.70765	2		35
FSHJ-49	Limestone (I)	Aramachay	623	− 0.3	− 6.5			0.70765	1		10
FSHJ-54	Limestone (I)	Condorsinga	664.5	− 2.4	− 7.0			0.70759	2		18
San Vicente											
FSV-473	Gypsum	Red Sandstone	− 30					0.70717	1		

Coarse calcite, Coarse-crystalline calcite; Repl. Dol, replacement dolomite; Sparry Dol, sparry dolomite; (I), original to moderately modified sedimentary rock; (II), late-diagenetic carbonate. The height is the distance above the Pucará-Mitu contact. The 2σ uncertainty is in the fifth decimal place of the $^{87}Sr/^{86}Sr$ ratio

regional replacement dolomite samples yield $^{87}Sr/^{86}Sr$ ratios that fall within or close to the range of seawater $^{87}Sr/^{86}Sr$ values published by Koepnick et al. (1990) for the Lower Jurassic and the Upper Triassic (Figs. 3, 4 and 5). The slight discrepancy between the Sr isotopic data of the limestone and evaporite samples from the Condorsinga Formation and the $^{87}Sr/^{86}Sr$ seawater curve may stem from the fact that the latter is only poorly constrained in the Lower Jurassic (Koepnick et al. 1990). Thus, our data indicate that the lower limit of the seawater curve may extend to lower $^{87}Sr/^{86}Sr$ ratios between the Hettangian and the Toarcian.

Two groups of carbonates yield distinctive Sr isotopic compositions that differ from seawater values: (1) carbonates near the basal contact with underlying detrital rocks show a progressive increase in $^{87}Sr/^{86}Sr$ ratios toward the base of the carbonate sequence; and (2) at the MVT deposits, ore-stage replacement dolomite and sparry carbonates are slightly enriched in ^{87}Sr with respect to Upper Triassic to Lower Jurassic seawater, with sparry carbonates being more enriched. The ^{87}Sr-enrichment is more important in the carbonates from the basal contact (Figs. 3 and 5).

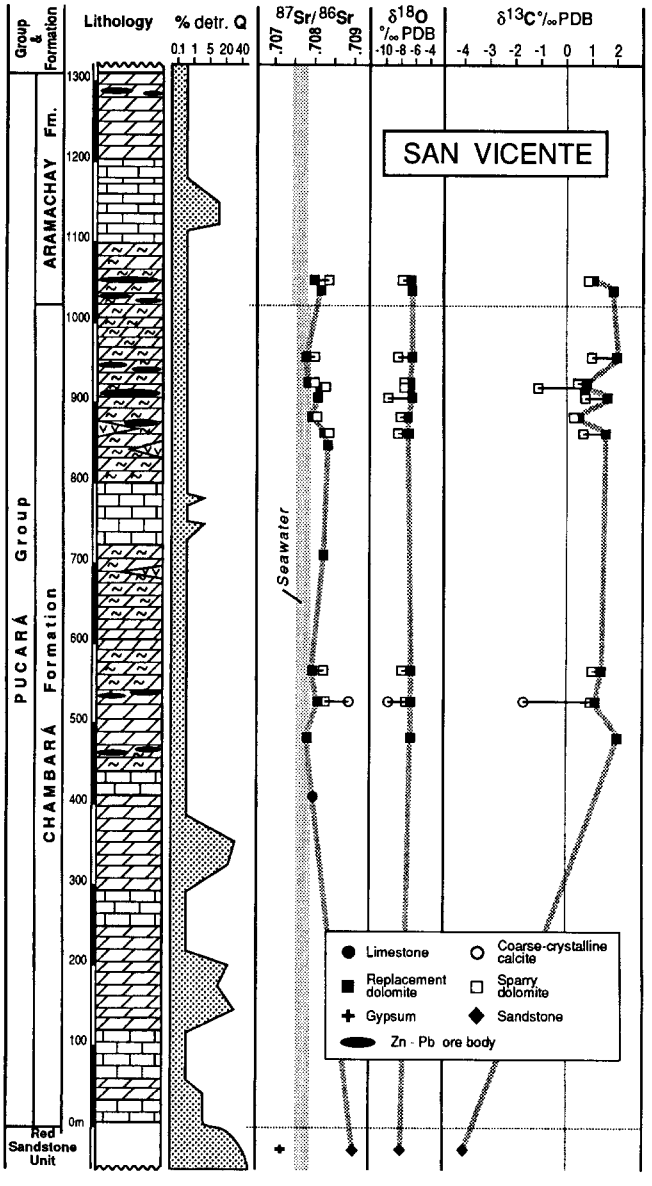

Fig. 4. Profile of part of the Pucará sequence at San Vicente with Sr, O and C isotopic trends. Isotope data from Fontboté and Gorzawski (1990)

Sources of strontium

Regional replacement dolomite remote from the Mitu-Pucará contact have Upper Triassic-Lower Jurassic seawater-like $^{87}Sr/^{86}Sr$ ratios. From this isotopic signature, it is inferred that seawater or precursor carbonates were ultimately the major source of Sr in the replacement dolomite emplaced regionally and remote from the Mitu-Pucará contact.

The ^{87}Sr-enrichment trends of the carbonate rocks at the MVT deposits and at the base of the Pucará basin indicate that their Sr is a mixture between Sr derived from the host rocks and Sr enriched in radiogenic ^{87}Sr. Potential sources of radiogenic ^{87}Sr are detrital and igneous silicate minerals with high Rb/Sr ratios. Given significant time, the decay of ^{87}Rb to ^{87}Sr will produce elevated $^{87}Sr/^{86}Sr$ ratios in these minerals. Release of radiogenic ^{87}Sr may occur as a result of albitization or dissolution of alkali feldspar, dissolution of mica, conversion of smectite to illite, and interlayer cation exchange (Chaudhuri 1978; Posey et al. 1987; Stueber et al. 1987; Chaudhuri and Clauer 1993).

A certain degree of elemental exchange between silicate and carbonate phases can be expected as a result of load pressure (Veizer and Compston 1974; Veizer 1989). Sparse detrital silicates interlayered with carbonates in the Pucará Group cannot be excluded entirely as a source for radiogenic ^{87}Sr. However, the trend displayed by the $^{87}Sr/^{86}Sr$ ratios of limestones and replacement dolomites does not correlate with the amount of detrital material interlayered within the Pucará Group (Figs. 3 and 4). Thus, detrital components within carbonate rocks of the Pucará Group must be ruled out as a significant source of radiogenic ^{87}Sr.

More realistically, the ^{87}Sr-enrichment trends of the carbonate rocks at the MVT deposits and at the base of the Pucará basin is explained by interaction of these rocks with ^{87}Sr-enriched fluids. Formation waters are commonly enriched in ^{87}Sr as a result of interaction with detrital and igneous silicate minerals. Given the systematic and gradual trend of increasing $^{87}Sr/^{86}Sr$ ratios toward the bottom of the Chambará Formation, the ^{87}Sr-rich fluid must have migrated upward into the latter, and the most likely source of radiogenic Sr is the underlying detrital rocks (Figs. 3, 4 and 5).

At low temperature (about $< 100\,^{\circ}C$), dissolution of plagioclase dominates the Sr isotopic composition of groundwaters in silicate rocks (Franklyn et al. 1991). In addition, reaction rates indicate that the Sr content of groundwaters in silicate rocks is affected at first by the dissolution of Ca-rich plagioclase, initially providing Sr with low $^{87}Sr/^{86}Sr$ ratios, followed by Na-rich plagioclase. With time the Sr isotopic ratios increase as alkali feldspar

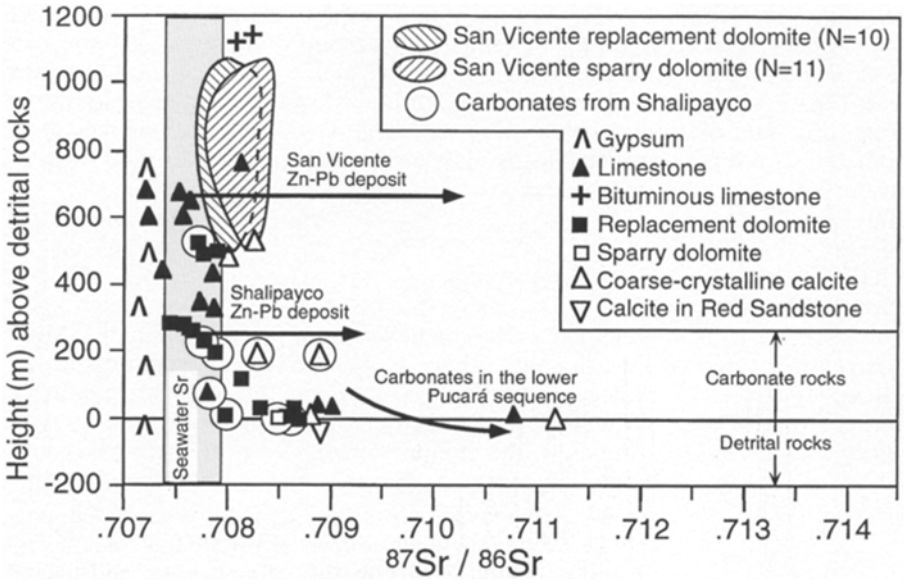

Fig. 5. Sampling height above contact between detrital rocks and carbonate rocks of the Pucará basin vs. $^{87}Sr/^{86}Sr$ ratios of the samples. San Vicente data are from Fontboté and Gorzawski (1990), and Upper Triassic to Lower Jurassic seawater Sr range is from Koepnick et al. (1990). The ratio obtained for NBS 987 in our laboratory is higher by 0.0001 than the one obtained by Koepnick et al. (1990) for NBS 987 (0.71014). Therefore, we have added the difference obtained on NBS 987 (0.0001) to their seawater curve. Since Fontboté and Gorzawski (1990) report a value of 0.710277 for NBS 987 similar, within analytical error, to the one obtained in our study, no corrections were made to their data used in this investigation

and mica become involved in the rock-water interaction process (Lasaga 1984; McNutt et al. 1990). Thus, particular attention has been given to specific mineral-water pairs in the following discussion, considering that MVT deposits form generally in an 80 °C to 150 °C temperature range (Bethke and Marshak 1990; Garven et al. 1993), a temperature range compatible with our preliminary fluid inclusion data from the San Vicente MVT deposit (see below).

Available isotopic data of various possible radiogenic ^{87}Sr source rock reservoirs in the study area are listed in Table 3. There are unfortunately no Sr isotope data for sedimentary and volcaniclastic rocks of the Mitu Group and the phyllites and quartzitic beds of the Excelsior Group, so that these sources cannot be evaluated adequately for their Sr isotopic signature. As stated previously, the MVT deposits were formed during the Late Cretaceous-Early Miocene, and most probably between the Late Eocene and Early Miocene. Thus, $^{87}Sr/^{86}Sr$ ratios have also been computed at 20, 40 and 100 Ma for the various source rocks listed in Table 3. Fluids with an $^{87}Sr/^{86}Sr$ ratio of at least 0.709 are required to explain the anomalous Sr isotopic composition of the carbonate rocks at the base of most of the Pucará Group, and fluids with an exceptionally high $^{87}Sr/^{86}Sr$ ratio of 0.7112 at Tingocancha (Figs. 2 and 3). At the MVT deposits, fluids with a $^{87}Sr/^{86}Sr$ ratio near 0.7085 are necessary to explain the ^{87}Sr-enriched nature of some sparry carbonates.

From inspection of Table 3 we recognize that during most of the evolution of the Pucará basin, including the 20 to 100 Ma time span, Late Permian-Early Triassic intrusions, including the San Ramón granite, and their reworked equivalents in the clastic rocks of the Mitu Group (Capdevila et al. 1977; Mégard 1978) appear to be an adequate source reservoir for supplying Sr with a $^{87}Sr/^{86}Sr$ ratio in a 0.7085 to 0.7090 range, assuming that plagioclase (An_{30}) was a dominant Sr supplier to the brine (Table 3). Late Permian-Early Triassic intrusions, including the San Ramón granite, consist of variable proportions of strongly albitized alkali-feldspar quartz, albitized and sericitized plagioclase, biotite altered to white mica-prehnite-chlorite, and hornblende (Capdevila et al. 1977; Mégard 1978; Carlier et al. 1982; Kontak et al. 1985). These rocks contain adequate mineralogy with characteristic alterations that typically result in release of Sr to the interacting fluids (Chaudhuri and Clauer 1993).

By contrast, the Mitu Group alkaline volcanic rocks, consisting of plagioclase (An_{65}) and forsterite phenocrysts in a plagioclase-clinopyroxene-sanidine-opaque-glass-olivine matrix (Kontak et al. 1990), yield Sr with too low a $^{87}Sr/^{86}Sr$ ratio to be considered as a likely source reservoir during the entire evolution of the Pucará basin. However, this does not exclude the molasse-type sedimentary rocks and volcaniclastic rocks of the Mitu Group as possible suppliers of radiogenic ^{87}Sr, in particular at Shalipayco.

In the eastern part of the basin (Fig. 2), the Brazilian Shield and its clastic derivatives (Lower Sarayaquillo Formation or Red Sandstone unit) must also be considered as a possible source of radiogenic ^{87}Sr. Calculations in Table 3 show that an initial $^{87}Sr/^{86}Sr$ ratio of about 0.708 is required at 600 Ma for these Precambrian rocks to be an adequate Sr source with a $^{87}Sr/^{86}Sr$ ratio between 0.7085 and 0.7090 at 20–100 Ma. Such an initial ratio of 0.708 is a conservative and realistic estimate, but further Sr isotopic studies of the Precambrian rocks are necessary to constrain correctly the potential role of the nearby Brazilian shield as a source of Sr. $^{87}Sr/^{86}Sr$ ratios up to 0.7112 in the lowermost carbonate rocks at Tingocancha in the western part of the basin remains anomalous with respect to the aformentioned sources. A possible explanation is that phyllites of the Excelsior Group, or local intrusive bodies (Lyons 1968) in this part of the basin have a mineralogical assemblage with particularly high $^{87}Sr/^{86}Sr$ ratios.

Nature of fluid movement

A regional-scale model of brine migration is required to explain the elevated $^{87}Sr/^{86}Sr$ ratios of the carbonates at

Table 3. Isotopic composition of potential sources of radiogenic Sr in lithologies underlying the Pucará basin

	Present-day $^{87}Sr/^{86}Sr$	Present-day $^{87}Rb/^{86}Sr$	Age (Ma) and dating method	Initial $^{87}Sr/^{86}Sr$	$^{87}Sr/^{86}Sr$ at 100 Ma	$^{87}Sr/^{86}Sr$ at 40 Ma	$^{87}Sr/^{86}Sr$ at 20 Ma	Data source
Mitu group alkali basalts	0.70663	0.6243	280 (K-Ar)	0.70414	0.70574	0.70627	0.70645	Kontak et al. (1990)
	0.70663	0.6243	245 (K-Ar)	0.70445	0.70574	0.70627	0.70645	Kontak et al. (1990)
Hypothetical K-feldspar		2.16	262.5	0.70430	0.70928	0.71112	0.71172	
Hypothetical plagioclase (An = 65)		0.05	262.5	0.70430	0.70442	0.70446	0.70447	
Permo-Triassic granitic intrusions:								
San Ramon granite (gray facies)	0.7210	3.59	246 (Rb-Sr)	0.70844	0.71590	0.71896	0.71998	Capdevila et al. (1977)
San Ramon granite (gray facies)	0.7299	6.38	246 (Rb-Sr)	0.70754	0.72080	0.72624	0.72805	Capdevila et al. (1977)
San Ramon granite (red facies)	0.7480	11.4	246 (Rb-Sr)	0.70811	0.73180	0.74153	0.74476	Capdevila et al. (1977)
Hypothetical plagioclase (An = 30)		0.085	246	0.70800	0.70818	0.70825	0.70827	
Calculations of theoretical Sr isotopic composition of the Precambrian basement (Brazilian shield)			600 (U-Pb)					Mégard (1987)
Whole rock		0.2	600	0.708	0.7094	0.7096	0.7097	
Plagioclase (An = 50)		0.085	600	0.708	0.7086	0.7087	0.7087	
K-feldspar		2.16	600	0.708	0.7234	0.7253	0.7259	
Mica		27	600	0.708	0.9007	0.9237	0.9314	

the MVT deposits within the Pucará sequence. The clastic rocks of the Mitu Group constitute the regional aquifer through which the brines migrated and acquired their elevated $^{87}Sr/^{86}Sr$ ratios. Steeply dipping faults in the eastern part of the basin (Fig. 2) are conceivable channel ways for fluid migration from the deeper clastic rocks upward into the stratigraphic column of the Pucará Group. Previous studies on MVT deposits have stressed the importance of faults as favorable channel ways to move warm, metal-bearing brines from regional aquifers to the site of ore deposition (Pélissonnier 1967; Clendenin and Duane 1990). Such a scenario implies most likely that brine migration was driven by tectonic compression or topography (see Bethke and Marshak 1990; Garven et al. 1993) during the Andean orogeny, with steeply dipping faults pumping fluids from depth (see Sibson et al. 1975). Such an interpretation is in line with the Pb isotope signatures of galenas from the MVT deposits, which indicate that the most likely sources of Pb are the volcaniclastic rocks of the Mitu Group at Shalipayco, and clastic rocks underlying the carbonate rocks of the Pucará Group at San Vicente (Fontboté and Gorzawski 1990; Fontboté et al. 1990).

Stable isotope data

Results

The various groups of dolomite from the Pucará basin show well defined ranges of $\delta^{18}O$ values (Fig. 6): (1) regional replacement dolomite remote from the Mitu-Pucará contact and from any ore occurrence has $\delta^{18}O$ values between 0.1‰ and −3.4‰ (PDB); (2) samples from regional replacement dolomite near the contact with

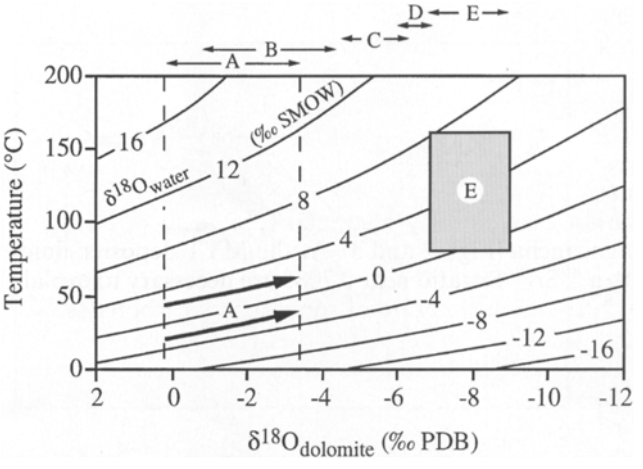

Fig. 6. $\delta^{18}O$ equilibrium between dolomite and water at varying temperatures of equilibration. Values for $\delta^{18}O$ in dolomitizing fluids calculated according to the equation of Land (1985): $\ln 10^3\ \alpha_{dolomite-fluid} = 2.78 \times 10^6 \times T^{-2}(°K) + 0.91$. *A* evolutionary path during heating of seawater; *B* regional replacement dolomite in the lowermost Pucará Group; *C* ore-stage replacement dolomite at the Shalipayco MVT deposit, *D* ore-stage replacement dolomite at the San Vicente MVT deposit; *E* ore-stage sparry dolomite at the San Vicente MVT deposit. See text for details

the Mitu Group yield values between $-1.1‰$ and $-4.3‰$ (PDB); (3) ore-stage replacement dolomites at the Shalipayco and San Vicente MVT deposits ranges between $-4.6‰$ and $-6.3‰$, and between $-5.8‰$ and $-6.9‰$ (PDB), respectively; and (4) sparry dolomite from San Vicente has $\delta^{18}O$ values between $-6.8‰$ and $-9.0‰$ (PDB). Figure 7A shows that progressive depletion in ^{18}O of the carbonates in the Pucará basin is accompanied by a gradual decrease in $\delta^{13}C$ values.

Discussion

The progressive shift toward lower $\delta^{18}O$ values of replacement dolomite at the base of the Pucará basin, and of ore-stage replacement and sparry carbonates at the MVT deposits is attributed to a temperature increase of the fluids, possibly coupled with an increase of the $\delta^{18}O$ value of the fluids (Fig. 6). Since temperature increases with burial depth, the regional replacement dolomite from the lowermost part of the Pucará sequence (range B in Fig. 6) may have been precipitated from hotter fluids than the fluids that formed the regional replacement dolomite remote from the Mitu-Pucará contact, higher up in the stratigraphic column (range A in Fig. 6).

Preliminary fluid inclusion microthermometry on sparry dolomite from the San Vicente MVT deposit (range E in Fig. 6) yields a homogenization temperature range of 115 °C to 162 °C and salinities between 9.5 wt.% and 26 wt.% NaCl equivalent. These temperatures are consistent with a previous investigation on the same deposit by the Japan International Cooperation Agency

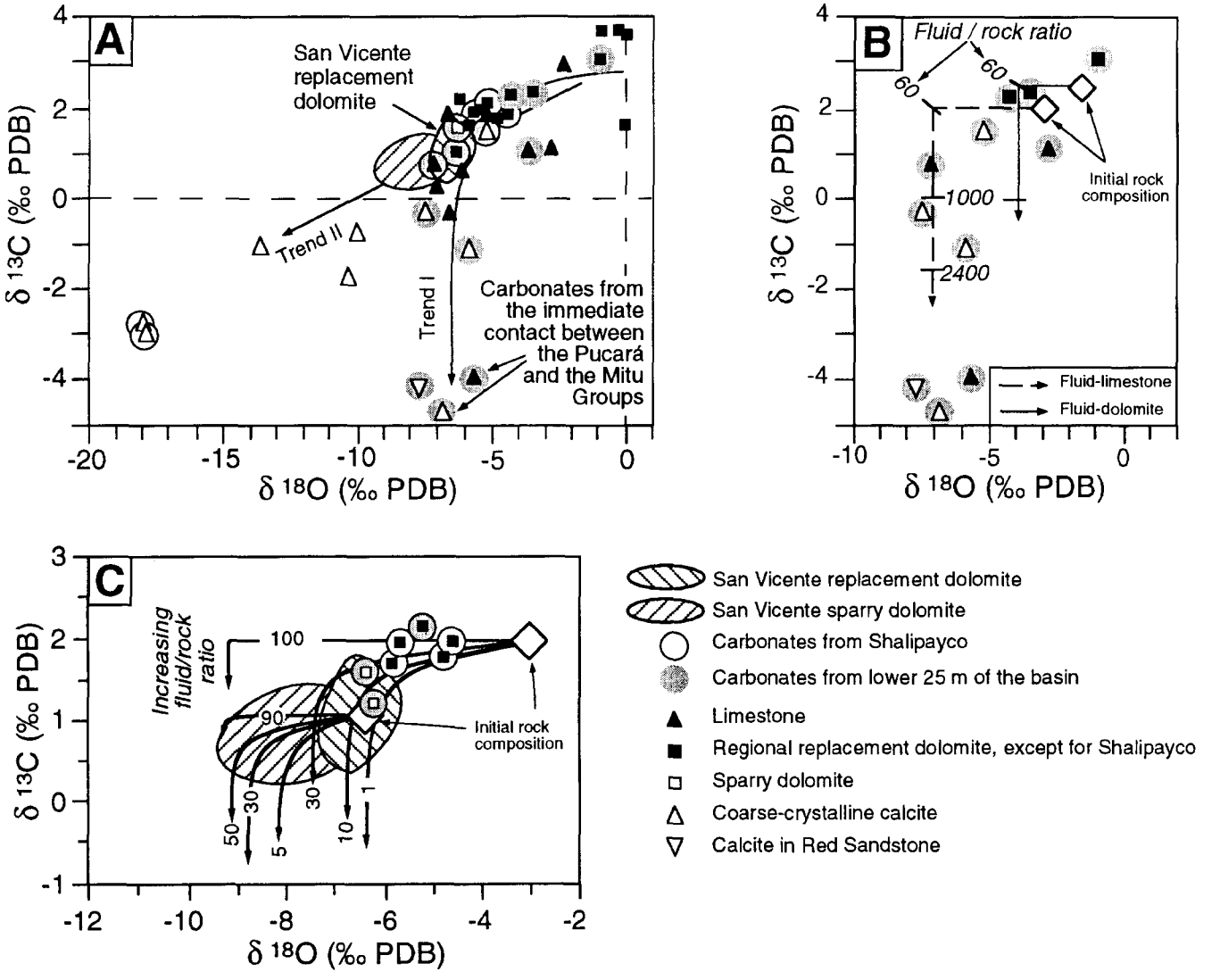

Fig. 7A–C. Covariation plots between $\delta^{13}C$ and $\delta^{18}O$ values of carbonates from the Pucará basin and results of quantitative calculations reproducing the covariation trends. San Vicente data are from Fontboté and Gorzawski (1990). **A** *Trend I* Covariation of carbonate rock data towards the lower part of the Pucará basin, *trend II* covariation of various carbonate generations at the MVT deposits; **B** modelling of the covariation trend of carbonates from the lowermost part of the Pucará basin. Note that quantitative calculations have been carried out for both fluid-limestone and fluid-dolomite interactions; **C** modelling of the covariation trend of the various dolomite generations from the MVT deposits. The *numbers* on the curve indicate the percentage of the high temperature, saline and radiogenic endmember (see fluid 2 in Table 5) in the fluid mixture interacting with the host rocks

(1976), reporting fluid inclusion homogenization temperatures between 70 °C and 140 °C, and sulfur isotope geothermometry by Fontboté and Gorzawski (1990) on sphalerite-galena pairs genetically associated with sparry dolomite, reporting a temperature range of 75 °C to 92 °C. The combined data tend to indicate that sparry dolomite in the MVT deposits was precipitated by a warm saline brine. This conclusion is in line with the general consensus that sparry, or saddle dolomite is typically formed by warm to hot saline fluids during diagenesis (e.g., Radtke and Mathis 1980; Machel 1987; Mountjoy et al. 1992; Shelton et al. 1992).

The box labeled E in Fig. 6 shows the oxygen isotopic composition of fluids in equilibrium with San Vicente sparry dolomite having $\delta^{18}O$ values between $-6.8‰$ and $-9.0‰$ (PDB) within a temperature range of 80 °C to 160 °C. This shows that the ore-bearing fluids had $\delta^{18}O$ values equal to or greater than 0‰ (SMOW). The increase in $\delta^{18}O$ values of the fluids concomitantly with temperature can be explained by isotopic exchange with clay minerals and carbonate rocks, and transformation of organic matter during burial diagenesis (Suchecki and Land 1983; Sheppard 1986; Longstaffe 1987). Finally, because there is such an intimate relationship between ore-stage replacement dolomite and sparry carbonates at the MVT deposits, it is unlikely that the fluids in equilibrium with ore-stage replacement dolomite had $\delta^{18}O$ values much below 0‰ (ranges C and D in Fig. 6).

In contrast to the oxygen isotopic trend, the decrease in $\delta^{13}C$ values (Fig. 7A) is due principally to a change in the isotopic composition of the carbon reservoir, because variation in temperature generally has a small effect on carbon isotope fractionation (Emrich et al. 1970). The tendency toward lower $\delta^{13}C$ values with paragenetic sequence possibly indicates that some carbon in ore-stage replacement and sparry carbonates at the MVT deposits was derived from organic matter. Degradation of organic matter is known as a likely process for decreasing $\delta^{13}C$ values of formation waters (Carothers and Kharaka 1980).

Nature of the fluids and mixing processes

Simultaneous changes in elemental abundances, and radiogenic and stable isotopic compositions of carbonates may reveal diagnostic trends in covariation diagrams which, together with quantitative modelling, place limitations on the nature of precipitating fluids and geochemical processes involved in carbonate diagenesis and ore-formation in sedimentary basins, including water-rock interaction and fluid mixing (Meyers 1989; Banner and Hanson 1990; Farr 1992; Zheng and Hoefs 1993). $\delta^{13}C$–$\delta^{18}O$ and $^{87}Sr/^{86}Sr$–$\delta^{18}O$ covariations of various carbonates from the Pucará basin are presented in Figs. 7 and 8, respectively. The marked increase in $^{87}Sr/^{86}Sr$ ratios of the barren carbonates toward the lower part of the Pucará basin is accompanied by a slight shift toward lower $\delta^{18}O$ values (Trend I in Fig. 8A), whereas the slight enrichment of ^{87}Sr in the various carbonate generations at the San Vicente deposit is accompanied by a larger depletion in ^{18}O (Trend II in Fig. 8A). Carbonate data from the Shalipayco deposit fall in between these two trends. In the $\delta^{13}C$ versus $\delta^{18}O$ diagram, carbonates from the MVT deposits display a broadly linear correlation with a positive slope (Trend II in Fig. 7A); by contrast, the stable isotopic data of carbonates from the base of the Pucará sequence yield a roughly inverted L-shaped trend (Trend I in Fig. 7A). Insofar as the ^{87}Sr-enrichment in carbonates from the base of the Pucará sequence and from the MVT deposits is attributed to a fluid ingress from underlying detrital rocks, an explanation is required to account for the different isotopic covariation trends.

We have used the approach suggested by Banner and Hanson (1990) to model the isotopic covariation trends. Mass-balance equations calculating simultaneous changes in elemental abundances and isotopic compositions during fluid-rock interaction in sedimentary systems allow us to compute diagnostic covariation trends which can be compared directly to a geochemical data set from a particular suite of samples. The advantage of such an approach is that only relative values are required for distribution coefficients, rock porosity, fluid salinities, fractionation factors, etc., in order to evaluate the relative importance of geochemical mixing processes. Moreover, the model curves are independent of absolute fluid-rock ratios, a further advantage since fluid-rock ratios determined by mass-balance methods may not be directly relevant to natural diagenetic systems (Baumgartner and Rumble 1988). The quantitative modelling of Banner and Hanson (1990) is an iterative calculation process. Fluid infiltration through a given rock volume is simulated by passing successive increments of fluid into available porosity, with each fluid increment reacting with the rock until isotopic equilibrium is achieved before it is displaced by the next increment of unreacted fluid. However, application of these calculations does not require that the mineral or rock phases have reached chemical equilibrium with the incoming fluid. In most situations, it is adequate to recognize that the mineral or rock composition has advanced toward equilibrium during the fluid-rock interaction process (Banner and Hanson 1990).

The isotopic trends of carbonates of the lowermost Pucará Group in the $\delta^{13}C$ versus $\delta^{18}O$ and $^{87}Sr/^{86}Sr$ versus $\delta^{18}O$ diagrams (trend I in Figs. 7B and 8B) were simulated by considering a single fluid-rock interaction model. It is assumed that a fluid with a homogeneous composition is derived from sedimentary clastic, volcaniclastic, volcanic and plutonic rocks underlying the Pucará carbonate rock sequence. Two different initial rock compositions were assumed, based on limestone and dolomite compositions sampled regionally and remote from the Mitu-Pucará contact and from ore occurrences (Table 4). Our calculations show that an interaction between these carbonate rocks and a moderately saline fluid with the characteristics given in Table 4 allows us to reproduce the isotopic covariation trends in the $\delta^{13}C$–$\delta^{18}O$ and $^{87}Sr/^{86}Sr$–$\delta^{18}O$ diagrams (Figs. 7B and 8B). The fluid used in our calculations has a moderate total dissolved carbon content (50 ppm C), and $\delta^{18}O$ and $\delta^{13}C$ values ($4‰$ SMOW and $-5‰$ PDB, respectively) that are consistent with the composition of deep formation waters (Carothers and Kharaka 1980; Suchecki and Land 1983). A $\delta^{18}O$ value of 4‰ (SMOW) is in concordance with the previous discussion of the evolution of oxygen isotopic

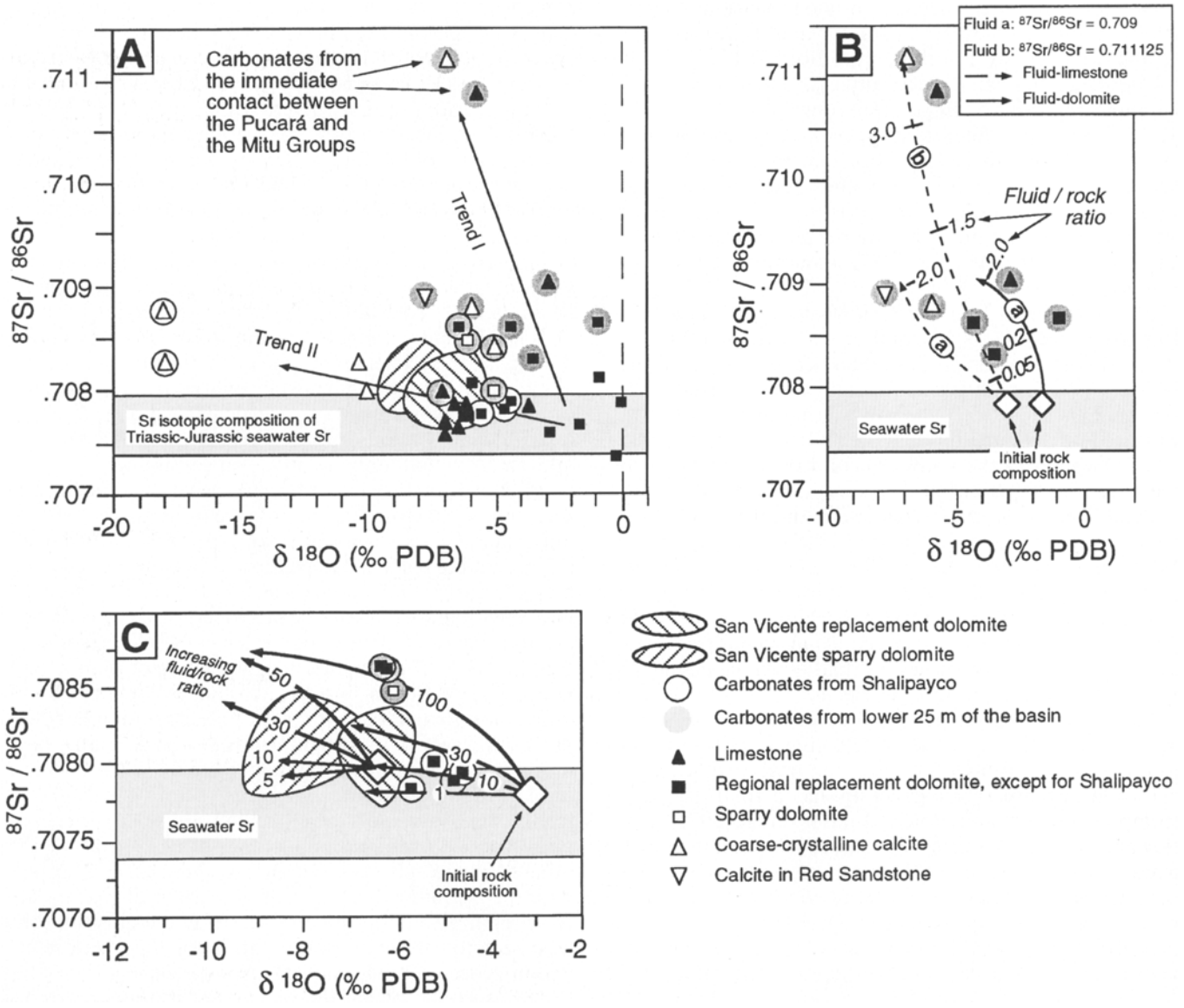

Fig. 8A–C. Covariation plots between $^{87}Sr/^{86}Sr$ ratios and $\delta^{18}O$ values of carbonates from the Pucará basin and results of quantitative calculations reproducing the covariation trends. San Vicente data are from Fontboté and Gorzawski (1990), and Upper Triassic to Lower Jurassic seawater Sr range is from Koepnick et al. (1990). **A** *Trend I* Covariation of carbonate rock data towards the lower part of the Pucará basin, *trend II* covariation of various carbonate generations at the MVT deposits; **B** modelling of the covariation trend of carbonates from the lowermost part of the Pucará basin. Note that quantitative calculations have been carried out for both fluid-limestone and fluid-dolomite interactions, and for both moderately (*fluid a*) and highly (*fluid b*) ^{87}Sr-enriched fluids; **C** modelling of the covariation trend of the various dolomite generations from the MVT deposits. The *numbers* on the curve indicate the percentage of the high temperature, saline and radiogenic endmember (see fluid 2 in Table 5) in the fluid mixture interacting with the host rocks

compositions of the fluids in the Pucará basin, and a $\delta^{13}C$ value of $-5‰$ (PDB) agrees with the lowest $\delta^{13}C$ value of carbonates at the immediate Mitu-Pucará contact (Fig. 7A).

Calculations were carried out using a moderately radiogenic fluid (A: $^{87}Sr/^{86}Sr = 0.709$), and with a highly radiogenic fluid (B: $^{87}Sr/^{86}Sr = 0.711125$) to account for the highly ^{87}Sr-enriched signature of the lowermost carbonates at Tingocancha (Fig. 3A). The fluid temperature in Table 4 was selected based on the assumption that the fluid-interaction process takes place at a depth of 2 to 3 km under a nearly normal geothermal gradient, and that the fluid is close to thermal equilibrium with the host rocks. Our knowledge about calcite-water and dolomite-water exchange distribution coefficients for Sr is still a matter of debate (Veizer 1983; Vahrenkamp and Swart 1990). However, as stated by Banner and Hanson (1990), a knowledge of precise distribution coefficients is not necessary in the computer simulations, since fluid-rock interaction trends in such diagrams as $^{87}Sr/^{86}Sr$ versus $\delta^{18}O$ are fairly independent of the absolute distribution coefficients over an order of magnitude range. Thus,

Table 4. Fluid and rock data for modelling the isotopic trends of the carbonate rocks at the bottom of the Pucará basin

Fluid composition:	A	B
$^{87}Sr/^{86}Sr$	0.70900	0.711125
$\delta^{18}O$ (‰, SMOW)	4	4
$\delta^{13}C$ (‰, PDB)	− 5	− 5
Sr (ppm)	325	325
Ca (ppm)	20000	20000
Total dissolved carbon (ppm C)	50	50
Temperature (°C)	78	78
Initial rock compositions:	Limestone	Dolomite
$^{87}Sr/^{86}Sr$	0.70778	0.70778
$\delta^{18}O$ (‰, PDB)	− 3.0	− 1.5
$\delta^{13}C$ (‰, PDB)	2.0	2.5
Sr (ppm)	250	48

a conservative exchange distribution coefficient estimate for Sr of 0.05 was used in our calculations. For the rock porosity we selected a value of 15%. For oxygen isotopes, we used the relationship $\Delta_{calcite-H_2O} = 2.78 \times 10^6 \times T^{-2} - 2.89$ (Friedman and O'Neil 1977), and the relationship $\Delta_{dolomite-calcite} = 3.8$ as discussed by Land (1985). For carbon isotopes, we used $\Delta_{calcite-HCO_3^-} = -8.914 \times 10^8 \times T^{-3} + 10.717 \times 10^6 \times T^{-2} - 38.27 \times 10^3 \times T^{-1} + 43.97$ and $\Delta_{dolomite-HCO_3^-} = -8.914 \times 10^8 \times T^{-3} + 10.897 \times 10^6 \times T^{-2} - 38.27 \times 10^3 \times T^{-1} + 44.14$ calculated from the equilibrium fractionation factors given in Ohmoto and Rye (1979, p. 551), where T is the temperature in degrees K.

The calculations have allowed us to reproduce the important enrichment in ^{87}Sr in the lowermost carbonate rocks in the Pucará basin compared to the initial rock compositions, with $\delta^{18}O$ values being only slightly shifted toward lower values (Fig. 8B). Although cumulative fluid-rock ratios should be considered only qualitatively, we can recognize logically in Figs. 7B and 8B that the cumulative fluid-rock ratios increase with proximity to the Mitu-Pucará contact. Furthermore, Fig. 7B shows that $\delta^{18}O$ values of both limestone and dolomite decrease gradually with progressive fluid-rock interaction while $\delta^{13}C$ values remain unchanged until high cumulative fluid-rock ratios are reached, at which stage $\delta^{13}C$ values of the carbonate rocks start to decrease. Such an inverted L-shaped trend is the result of the high oxygen to carbon ratio in water relative to carbonate rocks (see Table 2 in Banner and Hanson 1990).

In order to reproduce the isotopic covariation trends of the various carbonate generations at the MVT deposits we must consider a range in fluid compositions. Our calculations (Figs. 7C and 8C) indicate that the mineralizing fluids reacting with the host rocks at the MVT deposits were mixtures between a low temperature and dilute endmember (fluid 1 in Table 5) and a high temperature, saline and radiogenic endmember (fluid 2 in Table 5). The latter is comparable in composition to the fluid that has produced the ^{87}Sr-enriched carbonate rocks in the lowermost Pucará basin. However, this fluid has a higher temperature and a slightly less radiogenic nature which can be related to temperature increase with advancing diagenesis and to interaction of the radiogenic fluid from the underlying detrital rocks with comparatively ^{87}Sr-depleted carbonate rocks of the Pucará sequence.

Table 5. Fluid and rock data for modelling the isotopic trends of ore-stage replacement dolomite and sparry dolomite from MVT deposits in the Pucará basin

Fluid compositions:	Low temperature, dilute, non-radiogenic end member (fluid 1)	High temperature, saline, radiogenic end-member (fluid 2)
$^{87}Sr/^{86}Sr$	0.70780	0.70875
$\delta^{18}O$ (‰, SMOW)	0	4
$\delta^{13}C$ (‰, PDB)	− 5 to − 25	− 5
Sr (ppm)	100	300
Ca (ppm)	2000	20000
Total dissolved carbon (ppm C)	50 to 2500	50
Temperature (°C)	72	140
Initial rock composition during precipitation of ore-stage replacement dolomite		
$^{87}Sr/^{86}Sr$	0.7078	
$\delta^{18}O$ (‰, PDB)	− 3	
$\delta^{13}C$ (‰, PDB)	2	
Sr (ppm)	50	

The calculated temperatures of the fluid are consistent with temperatures yielded by fluid inclusion microthermometry and sulfur isotope geothermometry at the San Vicente MVT deposit. The $\delta^{18}O$ values of the computed fluid mixtures interacting with the wallrocks during formation of ore-stage replacement dolomite and sparry dolomite are in a 0‰ to 4‰ (SMOW) range, thus compatible with fluid-dolomite $\delta^{18}O$ equilibrium in the inferred temperature range for formation of the MVT deposits (see box E in Fig. 6).

The range in fluid compositions necessary to reproduce the covariation trends is a function of the different stratigraphic positions of the MVT deposits. The Zn-Pb orebodies at Shalipayco are confined to the lower 500 m of the Pucará sequence (Fig. 3D), close to the source of radiogenic ^{87}Sr that is the underlying Mitu Group, whereas orebodies at San Vicente are mostly between 500 and 1100 m above the contact between detrital and carbonate rocks of the Pucará Group, just below the bituminous-rich lithological sequence of the Aramachay Formation (Fig. 4). Our calculations show that the isotopic covariation trend of the carbonates close to the Pucará-Mitu contact at Shalipayco is better reproduced by fluids dominated by a hot, radiogenic brine that had reacted with rocks of the underlying Mitu Group (fluid 2 in Table 5).

In contrast, the covariation trend of the carbonates higher in the stratigraphic sequence at Shalipayco is better reproduced by fluid mixtures dominated by the low temperature, dilute local brine (fluid 1 in Table 5). The latter also applies to the San Vicente deposit (Figs. 7C and 8C) with the difference that a much lower $\delta^{13}C$ value of − 25‰ (PDB) and a much higher total dissolved carbon content of 2500 ppm are required to model isotopic covariation trends of ore-related carbonates (Table 5). The low $\delta^{13}C$ value and high total dissolved carbon content in the local fluid are probably related to proximity of the

bituminous-rich sequence of the Aramachay Formation relative to orebodies at San Vicente.

To account for the stepped pattern in $\delta^{18}O$–$\delta^{13}C$ space (Fig. 7C) when progressing from ore-stage replacement dolomite to sparry dolomite at the San Vicente MVT deposit, fluid-rock interaction calculations were carried out in two steps. One initial rock composition was used at the very onset of fluid-rock interaction for the formation of ore-stage replacement dolomite, and in a second step, the average composition of the ore-stage replacement dolomite was computed to set the new initial rock compositions for producing sparry dolomite (Fig. 7C). This assumes that the host rock composition evolves during the fluid-interaction process and becomes enriched in ^{87}Sr and Sr, and depleted in ^{18}O and ^{13}C with time.

Conclusions

The isotopic compositions of limestone and replacement dolomite in the Pucará basin are mostly consistent with Upper Triassic to Lower Jurassic marine carbonates. Our data indicate that the Sr isotopic composition of seawater between the Hettangian and the Toarcian may extend to lower $^{87}Sr/^{86}Sr$ ratios than previously published values.

Two carbonate groups in the Pucará basin are enriched in ^{87}Sr: (1) at the basin scale, $^{87}Sr/^{86}Sr$ ratios of limestone, replacement dolomite and late stage coarse-crystalline calcite increase gradually toward the contact between carbonate rocks and underlying detrital lithologies; and (2) ore-stage replacement dolomite and sparry carbonates from MVT deposits also show a slight enrichment in ^{87}Sr with respect to carbonate rocks from barren areas. The elevated $^{87}Sr/^{86}Sr$ ratios are attributed to an interaction of the carbonate rocks with incoming brines enriched in ^{87}Sr due to interaction with underlying lithologies rich in silicate minerals.

A rigorous assessment of the Sr source is not possible at the present time due to a lack of a comprehensive isotopic record of the possible source rock reservoirs. Nevertheless, calculations show that the San Ramón granite, or other similar Permo-Triassic intrusions, and their clastic derivatives in the Mitu group are a likely source of ^{87}Sr. Additional possible sources of radiogenic Sr are sedimentary and volcaniclastic rocks of the Mitu Group, and the Brazilian shield and its erosion products, provided that the Precambrian rocks had an initial $^{87}Sr/^{86}Sr$ ratio of or greater than 0.708 around 600 Ma. However, volcanic rocks of the Mitu Group had too low a $^{87}Sr/^{86}Sr$ ratio during the entire evolution of the Pucará basin for providing the radiogenic ^{87}Sr necessary for the ^{87}Sr-enrichment in carbonates in the lower part of the basin and in the MVT deposits. However, molasse-type sedimentary rocks and volcaniclastic rocks of the Mitu Group could be possible suppliers of radiogenic ^{87}Sr, in particular at Shalipayco.

The regional marked enrichment in ^{87}Sr of carbonates toward the lower part of the Pucará Group is accompanied by only a slight decrease in $\delta^{18}O$ values and essentially no change in $\delta^{13}C$ values. By contrast, replacement dolomite and sparry carbonates at the MVT deposits display a coherent trend of progressive ^{87}Sr-enrichment, and ^{18}O- and ^{13}C-depletion. For a given $\delta^{18}O$ value, the ^{87}Sr-enrichment is more important in the Shalipayco MVT deposit located in the lowermost part of the Pucará sequence, than in the San Vicente MVT deposit which occurs higher in the stratigraphic sequence. The depletion in ^{18}O in replacement dolomite and sparry carbonates from MVT deposits is interpreted as indicating a temperature increase possibly coupled with an enrichment in ^{18}O of the ore-forming fluids. Progressively lower $\delta^{13}C$ values throughout the paragenetic sequence at the MVT deposits are interpreted as a gradually more important contribution from organically derived carbon.

The regional marked ^{87}Sr-enrichment and the slight decrease in $\delta^{18}O$ values in carbonate rocks from the lower part of the Pucará Group can be reproduced satisfactorily by a single fluid-rock interaction model, with a fluid that has reacted with the underlying detrital lithologies, and the composition of which is compatible with the one of deep formation waters. Isotopic covariation trends of the MVT deposits are also modelled satisfactorily by a fluid-rock interaction process. But in the latter case, the interacting fluids have a range of compositions representing mixtures of the hot, saline and radiogenic brine that has reacted with the underlying detrital lithologies and cooler, dilute brines possibly representing local fluids within the Pucará sequence. The composition of the local fluids varies according to the nature of the lithologies present in the neighborhood of the different MVT deposits. Moreover, the proportion of the radiogenic fluid derived from the detrital lithologies in the modelled fluid mixtures interacting with the carbonate host rocks at the MVT deposits decreases as one moves up in the stratigraphic sequence of the Pucará Group.

Acknowledgements. This study was supported by a grant to L. Fontboté and D. Fontignie from the Swiss National Science Foundation (Grant number 21.30.309.90). This is a contribution to IGCP project 342 (Age and Isotopes of South American Ores). The management and staff of CENTROMIN and SIMSA, Peru are gratefully acknowledged for support during field work at the Yauli and the Malpaso Domes, and at San Vicente. Ingeniero D. Ríos, Compañia Minera Huarón from Lima, and J. Merino are thanked for information about the Shalipayco deposit. The authors would like to thank M. Falceri and D.M. Yu (University of Geneva) for assistance and advice during the analytical part of this study. Thanks are also due J. Metzger (University of Geneva) for drafting most of the figures. M. Doppler (University of Geneva) is thanked for some sample preparation. Discussions with J.M. Martín and J.C. Braga (University of Granada) clarified sedimentological aspects of the Pucará basin. Critical reviews by Kevin Shelton and an anonymous reviewer helped us to clarify and improve the manuscript.

References

Al-Aasm, I.S., Taylor, B.E., South B. (1990) Stable isotope analysis of multiple carbonate samples using selective acid extraction. Chem. Geol. 80:119–125

Anderson, G.M., Macqueen, R.W. (1988) Mississippi Valley-type lead-zinc deposits. In: Roberts, R.G., Sheahan, P.A. (eds.) Ore deposit models. Geoscience Canada Reprint Series 3:79–90

Banner, J.L., Hanson, G.N. (1990) Calculation of simultaneous isotopic and trace element variations during water-rock interaction with applications to carbonate diagenesis. Geochim. Cosmochim. Acta 54:3123–3137

Bannner, J.L., Hanson, G.N., Meyers, W.J. (1988) Water-rock interaction history of regionally extensive dolomites of the Burlington-Keokuk Formation (Mississippian) : isotopic evidence. In: Shukla, V., Baker, P.A. (eds.) Sedimentology and geochemistry of Dolostones. Soc. Econ. Paleontologists Mineralogists Spec. Publ. 43:97–113

Baumgartner, L.P., Rumble, D. (1988) Transport of stable isotope. I. Development of a kinetic continuum theory for stable isotope transport. Contrib. Mineral. Petrol. 98:417–430

Beales, F.W., Hardy, J.L. (1980) Criteria for the recognition of diverse dolomite type with an emphasis on studies on host rocks for Mississippi Valley-Type ore deposits. In: Zenger, D.H., Dunham, J.B., Ethington, R.L. (eds.) Concepts and models of dolomitization. Soc. Econ. Paleontologists. Mineralogists Spec. Publ. 28:197–213

Bethke, C.M., Marshak, S. (1990) Brine migrations across North America – The plate tectonics of groundwater. Ann. Rev. Earth Planet. Sci. 18:287–315

Capdevila, R., Mégard, F., Paredes, J., Vidal P. (1977) Le batholite de San Ramón, cordillère orientale du Pérou central. Geol. Rundsc. 66:434–446

Carlier, G., Grandin, G., Laubacher, G., Marocco, R., Mégard, F. (1982) Present knowledge of the magmatic evolution of the Eastern Cordillera of Peru. Earth-Sci. Rev. 18:253–283

Carothers, W.W., Kharaka, Y.K. (1980) Stable carbon isotopes of HCO_3^- in oil-field waters-implications for the origin of CO_2. Geochim. Cosmochim. Acta 44:323–332

Chaudhuri, S. (1978) Strontium isotopic composition of several oil-field brines from Kansas and Colorado. Geochim. Cosmochim. Acta 42:329–331

Chaudhuri, S., Clauer, N. (1993) Strontium isotopic composition and potassium and rubidium contents of formation waters in sedimentary basins: clues to the origin of the solutes. Geochim. Cosmochim. acta 57:429–437

Clendenin, C.W., Duane, M.J. (1990) Focused fluid flow and Ozark Mississippi Valley-type deposits. Geology 18:116–119

Emrich, K., Erhalt, D.H., Vogel, J.C. (1970) Carbon isotope fractionation during the precipitation of calcium carbonate. Earth Planet. Sci. Lett. 8:363–371

Farr, M.R. (1992) Geochemical variation of dolomite cement within the Cambrian Bonneterre Formation, Missouri: evidence for fluid mixing. J. Sediment. Petrol. 62:636–651

Fontboté, L. (1990) Stratabound ore deposits in the Pucará basin. An overview. In: Fontboté, L., Amstutz, G.C., Cardozo, M., Cedillo, E., Frutos, J. (eds.) Stratabound ore deposits in the Andes. Springer, Berlin Heidelberg New York, pp. 253–266

Fontboté, L., Gorzawski, H. (1990) Genesis of the Mississippi Valley-type Zn-Pb deposit of San Vicente, Central Peru: geological and isotopic (Sr, O, C, S) evidences. Econ. Geol. 85:1402–1437

Fontboté, L., Gunnesch, K.A., Baumann, A. (1990) Metal sources in stratabound ore deposits in the Andes (Andean cycle) – Lead isotopic constraints. In: Fontboté, L., Amstutz, G.C., Cardozo, M., Cedillo, E., Frutos, J. (eds.) Stratabound ore deposits in the Andes. Springer, Berlin Heidelberg New York, pp. 759–773

Franklyn, M.T., McNutt, R.H., Kamineni, D.C., Gascoyne, M., Frape, S.K. (1991) Groundwater $^{87}Sr/^{86}Sr$ values in the Eye-Dashwa Lakes pluton, Canada: evidence for plagioclase-water reaction. Chem. Geol. 86:111–122

Friedman, I., O'Neil, J.R. (1977) Compilation of stable isotope fractionation factors of geochemical interest. In: Fleischer, M. (ed.) Data of Geochemistry. 6th edn. U.S. Geological Survey Professional Paper 440-KK, 12 pp

Garven, G., Gee, S., Person, M.A., Sverjensky, D.A. (1993) Genesis of stratabound ore deposits in the Midcontinent basins of North America. 1. The role of regional groundwater flow. Am. J. Sci. 293:497–568

Ghazban, F., Schwarcz, H.P., Ford, D.C. (1992) Multistage dolomitization in the Society Cliffs Formation, northern Baffin Island, Northwest Territories, Canada. Can. J. Earth Sci. 29:1459–1473

Gorzawski, H., Fontboté, L., Sureau, A., Calvez, J.Y. (1989) Strontium isotope trends during diagenesis in ore-bearing carbonate basins. Geol. Rundsc. 78:269–290

Japan International Cooperation Agency (1976) Report on geological survey of the Cordillera Oriental, central Peru. Unpublished report, Japan Mining Agency, Japan International Cooperation Agency, Lima, vol. 2, pp. 39–40

Kaufman, J., Meyers, W.J., Hanson, G.N. (1990) Burial cementation in the Swan Hills formation (Devonian), Rosevear field, Alberta, Canada. J. Sediment. Petrol 60:918–939

Kaufman, J., Hanson, G.N., Meyers, W.J. (1991) Dolomitization of the Devonian Swan Hills formation, Rosevear field, Alberta, Canada. Sedimentology 38:41–66

Kesler, S.E. (1994) Mississippi Valley-type deposits in continental margin basins: lessons from the Appalachian–Caledonian orogen. In: Fontboté, L., Boni, M. (eds.) Sediment-hosted Zn-Pb ores. Springer, Berlin Heidelberg New York, pp. 89–103

Kessen, K.M., Woodruff, M.S., Grant, N.K. (1981) Gangue mineral $^{87}Sr/^{86}Sr$ ratios and the origin of Mississippi Valley-Type mineralization. Econ. Geol. 76:913–920

Kobe, H.W. (1990) Stratabound sulfide occurrences in the Paleozoic of the Yauli Dome, central Peru. In: Fontboté, L., Amstutz, G.C., Cardozo, M., Cedillo, E., Frutos, J. (eds.) Stratabound ore deposits in the Andes. Springer, Berlin Heidelberg New York, pp. 113–127

Koepnick, R.B., Denison, R.E., Burke, W.H., Hetherington, E.A., Dahl, D.A. (1990) Construction of the Triassic and Jurassic portion of the Phanerozoic curve of seawater $^{87}Sr/^{86}Sr$. Chem. Geol. 80:327–349

Kontak, D.J., Clark, A.H., Farrar, E., Strong, D.F. (1985) The rift-associated Permo-Triassic magmatism of the Eastern Cordillera: a precursor to the Andean orogeny. In: Pitcher, W.S., Atherton, M.P., Cobbong, E.J., Beckinsale, R.D. (eds.) Magmatism at a plate edge. Blackie, Glasgow and London, pp. 36–44

Kontak, D.J., Clark, A.H., Farrar, E., Archibald, D.A., Baadsgaard, H. (1990) Late Paleozoic-early Mesozoic magmatism in the Cordillera de Carabaya, Puno, southeastern Peru: geochronology and petrogeochemistry. J. South Am. Earth Sci. 3:213–230

Land, L.S. (1985) The origin of massive dolomite. J. Geol. Educ. 33:112–125

Lasaga, A.C. (1984) Chemical kinetics of water-rock interactions. J. Geophys. Res. B89:4009–4025

Leach, D.L., Rowan, E.L. (1986) Genetic link between Ouachita foldbelt tectonism and the Mississippi Valley-type lead-zinc deposits of the Ozarks. Geology 14:931–935

Longstaffe, F.J. (1987) Stable isotope studies of diagenetic processes. In: Kyser, T.K. (ed.) Stable isotope geochemistry of low temperature fluids. Mineral. Assoc. Can. Short Course 13:187–257

Loughman, D.L., Hallam, A. (1982) A facies analysis of the Pucará Group (Norian to Toarcian carbonates, organic-rich shale and phosphate) of central and northern Perú. Sediment. Geol. 32:161–194

Lyons, W.A. (1968) The geology of the Carahuacra mine, Peru. Econ. Geol. 63:247–256

Machel, H.-G. (1987) Saddle dolomite as a by-product of chemical compaction and thermochemical sulfate reduction. Geology 15: 936–940

Machel, H.-G., Mountjoy, E.W. (1986) Chemistry and environments of dolomitization – A reappraisal. Earth Sci. Reviews 23: 172–222

McCrea, J.M. (1950) On the isotopic chemistry of carbonates and a paleotemperature scale. J. Chem. Physics 18:849–857

McNutt, R.H., Frape, Fritz, P., Jones, M.G., MacDonald, I.M. (1990). The $^{87}Sr/^{86}Sr$ values of Canadian Shield brines and fracture minerals with applications to groundwater mixing, fracture history, and geochronology. Geochim. Cosmochim. Acta 54:205–215

Mégard, F. (1978) Etude géologique des Andes du Pérou central. ORSTOM Mémoire 86:306 pp.

Mégard, F. (1987) Structure and evolution of the Peruvian Andes. In: Schaer, J.-P., Rodgers, J. (eds.) The anatomy of mountain ranges. Princeton University Press, Princeton, pp. 179–210

Meyers, W.J. (1989) Trace element and isotope geochemistry of zoned calcite cements, Lake Valley Formation (Mississippian, New Mexico): insights from water-rock inreaction modelling. Sediment. Geol. 65:355–370

Mountjoy, E.W., Qing, H., McNutt, R.H. (1992) Strontium isotopic composition of devonian dolomites, Western Canada Sedimentary Basin: significance of sources of dolomitizing fluids. Appl. Geochem. 7:59–75

Ohmoto, H., Rye, R.O. (1979) Isotopes of sulfur and carbon. In: Barnes, H.L. (ed.) Geochemistry of hydrothermal ore deposits. Wiley, New York, pp. 509–567

Pélissonnier, H. (1967) Analyse paléohydrologique des gisements stratiformes de plomb, zinc, baryte, fluorite du type "Mississippi Valley". In: Brown, J.S. (ed.) Genesis of stratiform lead-zinc-barite-fluorite deposits in carbonate rocks (The so-called Mississippi Valley type deposits). Econ. Geol. Monogr. 3:234–252

Posey, H.H., Kyle, J.R., Jackson, T.J., Hurst, S.D., Price, P.E. (1987) Multiple fluid components of salt diapirs and salt dome cap rocks, Gulf Coast, U.S.A. Appl. Geochem. 2:523–534

Prinz, P. (1985a) Stratigraphie und Ammonitenfauna der Pucará-Gruppe (Obertrias-Unterjura) von Nord-Perú. Paleontographica 188:153–197

Prinz, P. (1985b) Zur Stratigraphie und Ammonitenfauna der Pucará-Gruppe bei San Vicente: Dept. Junin, Perú. Newsl. Stratigr. 14:129–141

Radke, B.M., Mathis, R.L. (1980) On the formation and occurrence of saddle dolomite. J. Sediment. Petrol. 50:1149–1168

Rosas, S. (1994) Facies, diagenetic evolution, and sequence analysis along a SW-NE profile in the southern Pucará basin (Upper Triassic-Lower Jurassic), central Peru. Heidelberger Geowiss. Abh., Ruprecht-Karls-Universität, Heidelberg, Germany 80:337 pp

Rosenbaum, J., Sheppard, S.M. (1986) An isotopic study of siderites, dolomites and ankerites at high temperatures. Geochim. Cosmochim. Acta 50:1147–1150

Russel, R.D. (1977) A solution in closed form for the isotopic dilution analysis of strontium. Chem. Geol. 20:307–314

Sangster, D.F. (1990) Mississippi Valley-type and sedex lead-zinc deposits: a comparative examination. Trans. Inst. Min. Metall. 99:B21–B42

Shelton, K.L., Bauer, R.M., Gregg, J.M. (1992) Fluid inclusion studies of regionally extensive epigenetic dolomites, Bonneterre Formation (Cambrian), southeast Missouri lead district: evidence of multiple fluids during dolomitization and lead-zinc mineralization. Geol. Soc. Am. Bull. 104:675–683

Sheppard, S.M.F. (1986) Characterization and isotopic variations in natural waters. In: Valley, J.W., Taylor, H.P., Jr., O'Neil, J.R. (eds.) Stable isotopes in high temperature geological processes. Rev. Mineral. 16:165–183

Sibson, R.H., Moore, J.McM., Rankin, A.H. (1975) Seismic pumping – a hydrothermal fluid transport mechanism. J. Geol. Soc. London 131:653–659

Spangenberg, J. (1995) Geochemical (elemental and isotopic) constraints on the genesis of the Mississippi Valley-type zinc-lead deposit of San Vicente, central Peru. Terre & Environnement, Geneva, 1:123 pp

Stueber, A.M., Pushkar, P., Hetherington, E.A. (1987) A strontium isotopic study of formation waters from the Illinois basin, USA. Appl. Geochem. 2:477–494

Suchecki, R.K., Land, L.S. (1983) Isotopic geochemistry of burial-metamorphosed volcanogenic sediments, Great Valley sequence, northern California. Geochim. Cosmochim. Acta 47:1487–1499

Sverjensky, D.A. (1984) Oil field brines as ore-forming solutions. Econ. Geol. 79:23–37

Sverjensky, D.A. (1986) Genesis of Mississippi Valley-type lead-zinc deposits. Ann. Rev. Earth Planet. Sci. 14:177–199

Szekely, T.S., Grose, L.T. (1972) Stratigraphy of the carbonate black shale and phosphate of the Pucará Group (Upper Triassic-Lower Jurassic), central Andes, Perú. Geol. Soc. Am. Bull. 83:407–428

Vahrenkamp, V.C., Swart, P.K. (1990) New distribution coefficient for the incorporation of strontium into dolomite and its implications for the formation of ancient dolomites. Geology 18: 387–391

Veizer, J. (1983) Chemical diagenesis of carbonates: theory and applications of trace element technique. Soc. Econ. Paleontologists Mineralogists Short Course 10:3.1–3.100

Veizer, J. (1989) Strontium isotopes in seawater through time. Ann. Rev. Earth Planet. Sci. 17:141–167

Veizer, J., Compston, W. (1974) $^{87}Sr/^{86}Sr$ composition of seawater during the Phanerozoic. Geochim. Cosmochim. Acta 38: 1461–1484

Zheng, Y.-F., Hoefs, J. (1993) Carbon and oxygen isotopic covariations in hydrothermal calcites. Theoretical modeling on mixing processes and application to Pb-Zn deposits in the Harz Mountains, Germany, Mineral. Deposita 28:79–89

Editorial handling: K.L. Shelton